

Evolutionary Paths Underlying Flower Color Variation in *Antirrhinum*

Annabel C. Whibley,^{1*} Nicolas B. Langlade,^{1*} Christophe Andalo,² Andrew I. Hanna,³ Andrew Bangham,³ Christophe Thébaud,² Enrico Coen^{1†}

To understand evolutionary paths connecting diverse biological forms, we defined a three-dimensional genotypic space separating two flower color morphs of *Antirrhinum*. A hybrid zone between morphs showed a steep cline specifically at genes controlling flower color differences, indicating that these loci are under selection. *Antirrhinum* species with diverse floral phenotypes formed a U-shaped cloud within the genotypic space. We propose that this cloud defines an evolutionary path that allows flower color to evolve while circumventing less-adaptive regions. Hybridization between morphs located in different arms of the U-shaped path yields low-fitness genotypes, accounting for the observed steep clines at hybrid zones.

A prevalent metaphor for describing evolutionary processes is the adaptive landscape, commonly visualized in three dimensions as an undulating surface of fitness values over a two-dimensional (2D) space representing various genotypes (1, 2). Different species may be considered to be at separate peaks on the landscape or to lie along ridges of high fitness. The notion of peaks is favored by the incompatible adaptive features of species, whereas ridges are favored as a way of accounting for underlying adaptive continuity. More recently, it has been argued that the issue of peaks versus ridges is an artifact of low-dimensional visualizations of fitness spaces as landscapes (3). What seem like separate peaks in 3D landscapes may be connected by paths in higher dimensions: the higher the dimensionality, the more likely such connections exist. However, it has proved difficult to demonstrate these paths in nature because of the challenge of dealing with higher dimensional genotypic and phenotypic spaces. We address this issue by combining molecular, genetic, and computational approaches to analyze flower color variation in natural populations and species of *Antirrhinum*.

Southern Europe contains 17 to 28 *Antirrhinum* species and subspecies, the number depending on taxonomic criteria (4–7). Although the species display diverse morphologies and flower colors, they can be crossed with each other and with the model species *A. majus* to give fertile progeny, reflecting their recent evolutionary origin (8–10). In most cases, the species occupy nonoverlapping geographical regions, precluding natural hybridization. Hybrid zones arise where species or morphs come into

contact, as happens in a region of the Pyrenees for the yellow-flowered *A. m. striatum* and the magenta-flowered *A. m. pseudomajus* (Fig. 1A).

Previous studies on nine species from the *Antirrhinum* group identified several major loci involved in natural flower color variation (11–13). These include the linked *ROSEA* (*ROS*) and *ELUTA* (*EL*) loci, affecting the intensity and pattern of magenta anthocyanin pigment, and *SULFUREA* (*SULF*), affecting the distribution

of yellow aurone pigment. To test whether these loci were important for color differences between *A. m. striatum* and *A. m. pseudomajus*, we crossed the two morphs to *A. majus* lines of known genotype (Fig. 2A). The F1s derived from the magenta morph were all magenta. By contrast, the yellow morph failed to complement mutations in *ROS* and *SULF* (Fig. 2A). The yellow morph also gave progeny with reduced magenta pigmentation when crossed to wild type, with a pattern similar to that conferred by the dominant *EL* allele. Like *EL*, the dominant allele from the yellow morph was tightly linked to *ROS* (14) (two recombinants were recovered out of 1300 test-cross progeny). Thus, *A. m. pseudomajus* is likely *ROS el/ROS el*; *SULF/SULF*, whereas *A. m. striatum* is *ros EL/ros EL*; *sulf/sulf*.

To assess further the contribution of *ROS* *EL* and *SULF* alleles to flower color differences, we intercrossed the two morphs. F2 individuals had a range of flower colors that were scored for magenta and yellow on the basis of overall visual appearance (Fig. 2B). The distributions for color were consistent, with a single segregating locus of major effect controlling each component of flower color (Fig. 2C). Individuals with a high yellow score were

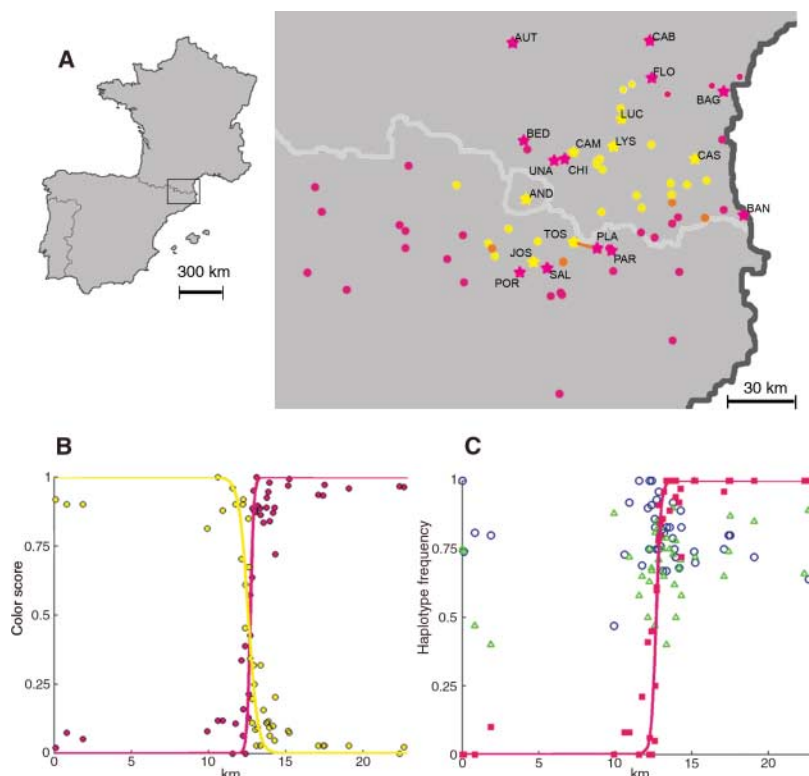


Fig. 1. Populations, phenotypes, and allele frequencies. (A) Location of the studied hybrid zone (orange line), other hybrid zones (orange circles), and sampled *A. m. pseudomajus* (magenta) and *A. m. striatum* (yellow) populations. Genetically studied populations are starred. (B) Clines in magenta and yellow color scores in subpopulations along a transect through the hybrid zone. (C) Frequencies of *ROS1* (magenta squares) and *PAL* (blue circles) haplogroups and a 6-base pair polymorphism at *DICH* (green triangles) in subpopulations along the hybrid zone transect. For *ROS1*, all markers were collapsed to a two-allele system.

¹Department of Cell and Developmental Biology, John Innes Centre, Colney Lane, Norwich NR4 7UH, UK.

²Laboratoire Evolution et Diversité Biologique, UMR 5174 CNRS–Université Paul Sabatier, 31062 Toulouse Cédex 9, France. ³School of Computing Sciences, University of East Anglia, Earlham Road, Norwich NR4 7TJ, UK.

*These authors contributed equally to this work.

†To whom correspondence should be addressed. E-mail: enrico.coen@bbsrc.ac.uk

sulf/sulf, whereas those with a low yellow score were either *SULF/SULF* or *SULF/sulf*, indicating that *SULF* genotype was the major determinant of variation in yellow. Individuals with a low magenta score were *ros EL/ros EL*, those with an intermediate score were *ROS el/ros EL*, and those with a high magenta score were *ROS el/ROS el*. Therefore, variation in magenta was largely accounted for by the *ROS EL* loci. These results allowed us to create an appropriate genotypic space for the F2. Digital images of representative flowers of four genotypes were warped to the same average flower shape. Principal component analysis on variation in pixel color at each position in the flower then allowed us to define a 3D genotypic space controlling flower color (15–17) (Fig. 2D).

The role of flower color variation in natural populations was assessed by analyzing a hybrid zone between *A. m. pseudomajus* and *A. m. striatum*. Scoring 493 plants across the hybrid zone revealed a steep cline for flower color (Fig. 1B). Allelism tests on 14 plants from the contact zone with a range of phenotypes confirmed that flower color was largely determined by *ROS*, *EL*, and *SULF* genotypes. For *ROS*, more extensive genotyping could be carried out by using molecular markers. The *ROS* locus comprises a tandem duplication of two MYB-related transcription factors, *ROS1* and *ROS2*, with *ROS1* having a greater role in flower color variation (13). We sequenced a 1.2-kb region of *ROS1*, from the promoter to the start of the second exon. Sequences from 13 yellow and 15 magenta morphs from locations distant from the contact zone showed that *ROS1* alleles fell into three major groups (haplogroups) (Fig. 3A). One haplogroup was specific to yellow morphs and was identical to the *ros^{dor}* allele of *A. majus*, hypothesized to have been derived from the wild (13). The other two haplogroups were found only in magenta morphs. *ROS1* sequences were used to design primers that allowed haplogroups to be distinguished by polymerase chain reaction. Genotyping 528 plants from the hybrid zone showed that the cline in *ROS1* haplogroup frequency coincided with magenta flower color (Fig. 1C).

Assuming that the hybrid zone arose from contact between previously separate yellow and magenta populations, the observed clines in flower color and genotype might have two explanations (18, 19). One is that *A. m. striatum* and *A. m. pseudomajus* came into recent contact and the clines reflect a neutral mixing of alleles between the populations. Alternatively, there has been a longer history of contact, and clines reflect selection maintaining morph differences. To evaluate these possibilities, we analyzed molecular variation at loci not involved in magenta and yellow morph differences. According to the neutral model, these loci should have a cline similar to that of *ROS1*. The *PALLIDA* (*PAL*) and *DICHOTOMA* (*DICH*) loci were chosen because they are linked to *ROS* [16

centimorgan (cM) and 9 cM from *ROS*, respectively], and sequences are available for primer design (20, 21). Alleles were sequenced from 18 individuals on either side of the hybrid zone. Most *PAL* alleles fell into two major haplogroups (Fig. 3B). *DICH* alleles showed little

haplogroup structure, although several DNA polymorphisms were detected. We genotyped 496 plants across the hybrid zone for the two *PAL* haplogroups and a polymorphism at *DICH*. No cline was observed for *PAL* or *DICH*, indicating that these genes were subject

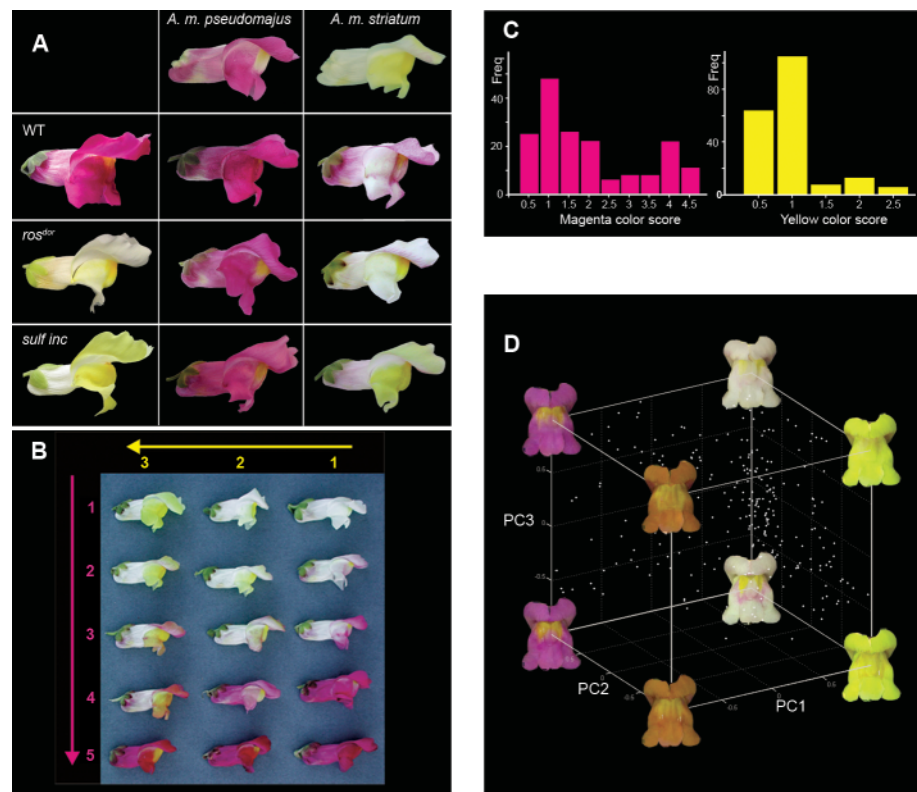


Fig. 2. Phenotypes and complementation tests. (A) F1 flowers from crosses between *A. m. pseudomajus* and *A. m. striatum* (top row) and cultivated *A. majus* genotypes (left column). *A. majus* homozygous lines are wild type (*ROS el; SULF*), *rosea^{dorsea}* (*ros^{dor} el; SULF*), and *sulfurea incolorata* (*ROS el; sulf; inc*). (B) Numerical scoring system for ranking magenta and yellow flower color. (C) Frequency of magenta (left) and yellow (right) scores in an F2 population from *A. m. striatum* × *A. m. pseudomajus*. (D) Genotypic space capturing flower color variation with three principal components (PCs). The four genotypes used for PC analysis were *ROS el/ROS el; SULF*–, *ros EL/ros EL; sulf/sulf*, *ROS el/ros EL; SULF*–, and *ros EL/ros EL; SULF*– (dash indicates unknown allele). Positions for 174 F2 and 110 F3 plants are shown as white points.

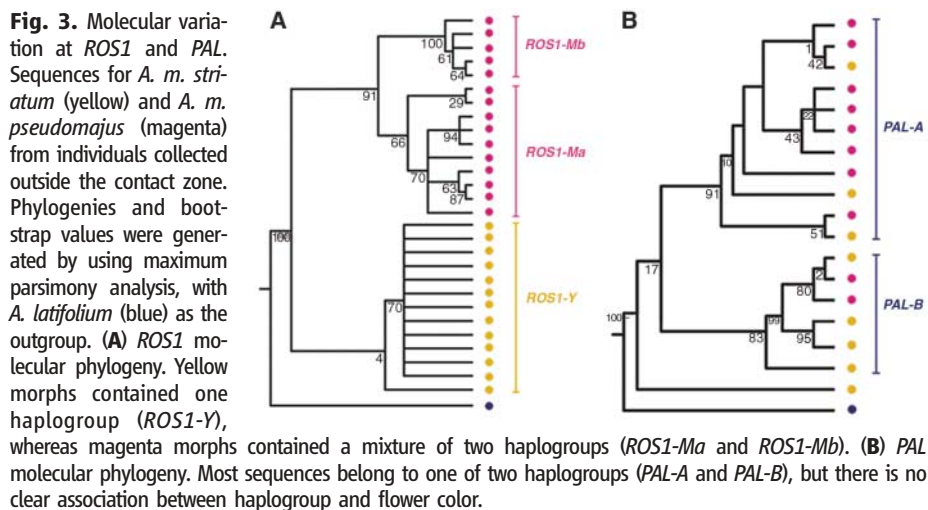


Fig. 3. Molecular variation at *ROS1* and *PAL*. Sequences for *A. m. striatum* (yellow) and *A. m. pseudomajus* (magenta) from individuals collected outside the contact zone. Phylogenies and bootstrap values were generated by using maximum parsimony analysis, with *A. latifolium* (blue) as the outgroup. (A) *ROS1* molecular phylogeny. Yellow morphs contained one haplogroup (*ROS1-Y*), whereas magenta morphs contained a mixture of two haplogroups (*ROS1-Ma* and *ROS1-Mb*). (B) *PAL* molecular phylogeny. Most sequences belong to one of two haplogroups (*PAL-A* and *PAL-B*), but there is no clear association between haplogroup and flower color.

to different evolutionary factors than *ROSI* (Fig. 1C). This was also supported by genotyping 16 *A. m. striatum* and *A. m. pseudomajus* populations distant from the hybrid zone (Fig. 1A and table S1). In all cases, the *ROSI* haplogroup correlated with flower color, whereas *PAL* and *DICH* loci showed no such association.

The simplest interpretation of these results is that spatial variation in *PAL* and *DICH* allele frequencies reflects historical gene flow between populations, whereas the *ROSI* cline has been maintained by selection on flower color. The cline could be maintained, for example, if intermediate genotypes have lower fitness than the parental morphs (22). Thus, magenta and yellow morphs might represent distinct peaks

on an adaptive landscape, whereas intermediate forms represent an intervening low fitness valley. However, this raises the problem of how the low fitness valley was traversed when the two morphs diverged from a common ancestor.

To address this issue, we mapped the range of phenotypes exhibited by *Antirrhinum* species within the defined genotypic space (Fig. 2D). This was achieved by photographing several flowers from each species (Fig. 4A) and warping the images to the same flower shape (Fig. 4B). We then determined the position in the genotypic space that best approximated the color for each flower (Fig. 4C). The approximation was evaluated by warping the resulting image back to the initial flower shape and comparing it to the original image (Fig. 4D). Much of the var-

iation in flower color was captured within the 3D genotypic space, consistent with previous studies showing that the *ROS*, *EL*, and *SULF* loci play important roles in color variation in the species group as a whole (11–13) (Fig. 4E).

When flowers from 19 species were mapped into the genotypic space, they collectively formed a broad U-shaped cloud of points (Fig. 4, F to H). Flowers from each species formed smaller clusters within this broader cloud. Magenta *A. m. pseudomajus* flowers localized near one end of the cloud, whereas yellow *A. m. striatum* flowers were near the other end. Intermediate positions within the cloud corresponded to various other patterns and intensities of color. However, certain color combinations were excluded from the cloud, even though they were observed in F2 and hybrid zone populations. For example, orange flowers, having a broad spread of both yellow and magenta (*ROS el/ROS el; sulf/sulf*), were not within the cloud (Fig. 4F). The absence of this genotype in wild species could be explained if individuals with orange flowers have lower fitness, perhaps because they are less attractive to pollinators (23–25). The role of pollinators in propagating *A. m. pseudomajus* and *A. m. striatum* is likely to be of central importance because the species are self-incompatible, seed dispersal is limited (involving gravity or water runoff), and individuals typically survive for only 1 to 3 years.

Taken together, our results suggest that magenta and yellow morphs did not evolve through intermediate genotypes giving orange flowers, but that instead evolution followed the route defined by the U-shaped cloud. According to this view, the cloud represents a region of high fitness, allowing flower color to evolve without incurring major fitness costs. However, when genotypes, such as magenta and yellow morphs, from distant parts of the cloud meet, they can generate progeny that lie outside the high fitness cloud, creating a barrier to exchange of flower color alleles. This would account for the observed steep cline at loci controlling color differences in the hybrid zone. A 2D slice through the U-shaped cloud, passing perpendicularly through its two arms, would yield an adaptive landscape with two separate peaks. The cloud therefore represents a high fitness path between what might otherwise seem like distinct peaks, showing how higher dimensional representations allow adaptive continuity and incompatibility to be more easily reconciled (2).

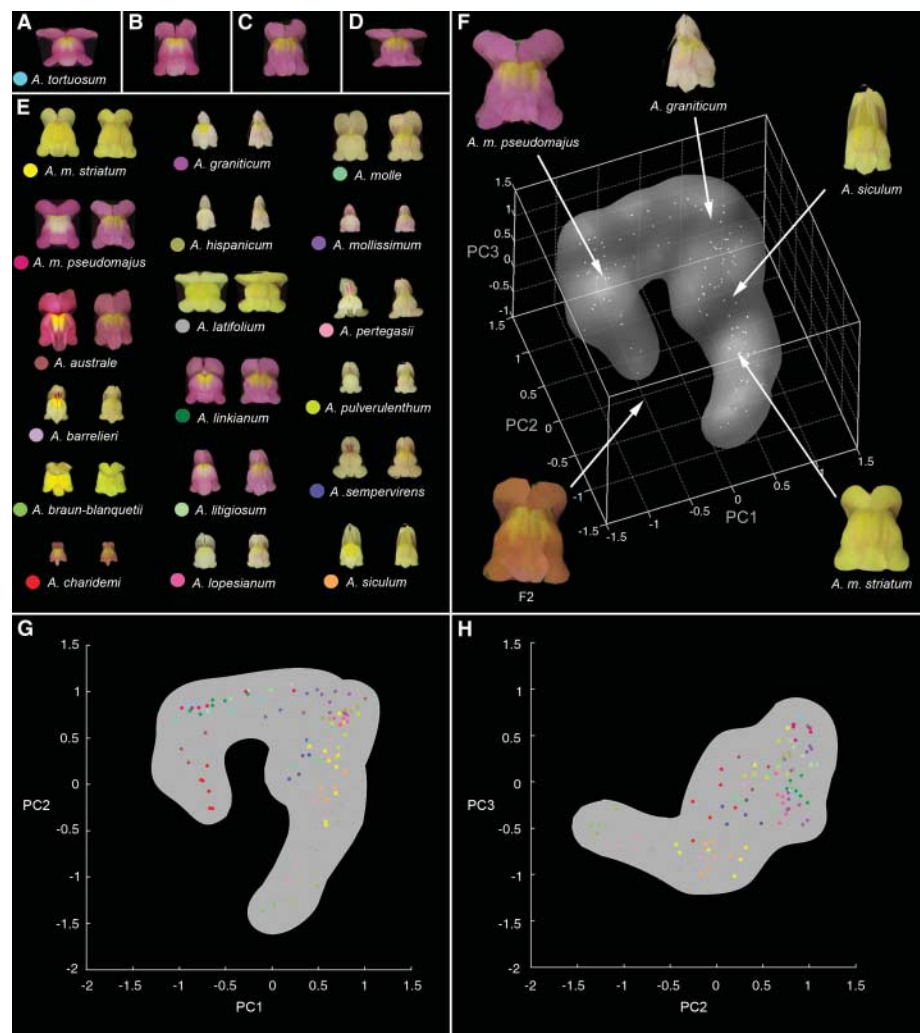


Fig. 4. *Antirrhinum* species placed in 3D genotypic space. (A) Mean *A. tortuosum* flower. (B) *A. tortuosum* flower warped to mean shape used to generate genotypic space (Fig. 1C). (C) Projection of (B) into genotypic space. (D) Image obtained when (C) is warped back to the mean *A. tortuosum* flower shape. (E) Projection of 19 *Antirrhinum* species into genotypic space. In each case, flower on the left shows the mean appearance, whereas flower on the right shows the appearance after projection into genotypic space [equivalent to (A) and (D) for each species]. (F) Cloud obtained for flowers from 19 species represented in genotypic space. Each point shows the position of a single flower projected into genotypic space. Examples of flowers from different positions in the genotypic space are illustrated. (G and H) Two different 2D projections of the cloud, with each species color-coded as in (E).

References and Notes

1. S. Wright, in Vol. 1 of *Proceedings of the Sixth Annual Congress of Genetics*, D. F. Jones, Ed. (Genetics Society of America, Austin, TX, 1932), p. 356–366.
2. S. Gavrilets, *Fitness Landscapes and the Origin of Species*, S. Levin, H. Horn, Eds., no. 41 of *Monographs in Population Biology* (Princeton Univ. Press, Princeton, NJ, 2004).
3. S. Gavrilets, *Trends Ecol. Evol.* **12**, 307 (1997).
4. W. Rothmaler, *Taxonomische Monographie der Gattung Antirrhinum* (Akademie-Verlag, Berlin, 1956).
5. D. A. Webb, in *Flora Europaea*, T. Tutin et al., Eds. (Cambridge Univ. Press, Cambridge, 1972), vol. 3.

6. D. Sutton, *A Revision of the Tribe Antirrhineae* (Oxford Univ. Press, Oxford, 1988).
7. I. Mateu-Andres, J. G. Segarra-Moragues, *Ann. Bot. (Lond.)* **92**, 647 (2003).
8. P. Vargas, J. A. Rosselló, R. Oyama, J. Güemes, *Plant Syst. Evol.* **249**, 151 (2004).
9. Z. Schwarz-Sommer, B. Davies, A. Hudson, *Nat. Rev. Genet.* **4**, 657 (2003).
10. T. Gubitz, A. Caldwell, A. Hudson, *Mol. Biol. Evol.* **20**, 1537 (2003).
11. J. Hackbarth, P. Michaelis, G. Scheller, *Z. Indukt. Abstammungs- Vererbungslehre* **80**, 1 (1942).
12. H. Stubbe, *Genetik und Zytologie von Antirrhinum L. sect. Antirrhinum* (Veb Gustav Fischer Verlag, Jena, Germany, 1966).
13. K. Schwinn *et al.*, *Plant Cell* **18**, 831 (2006).
14. E. Baur, *Bibl. Genet.* **4**, 1 (1924).
15. G. W. Horgan, *Comput. Electron. Agric.* **31**, 169 (2001).
16. T. F. Cootes, G. J. Edwards, C. J. Taylor, *IEEE Trans. Pattern Anal. Mach. Intell.* **23**, 681 (2001).
17. N. B. Langlade *et al.*, *Proc. Natl. Acad. Sci. U.S.A.* **102**, 10221 (2005).
18. N. H. Barton, G. M. Hewitt, *Annu. Rev. Ecol. Syst.* **16**, 113 (1985).
19. N. H. Barton, B. O. Bengtsson, *Heredity* **57**, 357 (1986).
20. D. Luo *et al.*, *Cell* **99**, 367 (1999).
21. E. S. Coen, R. Carpenter, C. Martin, *Cell* **47**, 285 (1986).
22. W. S. Moore, J. T. Price, in *Hybrid Zones and the Evolutionary Process*, R. G. Harrison, Ed. (Oxford Univ. Press, Oxford, 1993), pp. 196–225.
23. D. W. Schemske, H. D. Bradshaw Jr., *Proc. Natl. Acad. Sci. U.S.A.* **96**, 11910 (1999).
24. L. Chittka, J. D. Thomson, Eds., *Cognitive Ecology of Pollination* (Cambridge Univ. Press, Cambridge, 2001).
25. H. D. Bradshaw Jr., D. W. Schemske, *Nature* **426**, 176 (2003).
26. We thank C. Martin and J. Venail for providing the *ROS* sequence before publication; M. Burrus, L. Copsey,

J. Bowers, C. Cazettes-Vicedo, and Z.-L. Liu for their help with carrying out genotyping and genetics; M. Bernardet, M. Cruzan, and J. Leneveu for their help in the field; and G. Hewitt for helping to initiate this project. This research was funded by grants from the Biotechnology and Biological Sciences Research Council, UK. Sequences are deposited in GenBank; accession numbers DQ866629 to DQ866657 for *ROSEA1*, DQ866658 to DQ866676 for *PALLIDA*, and DQ866677 to DQ866701 for *DICHOTOMA*.

Supporting Online Material

www.sciencemag.org/cgi/content/full/313/5789/963/DC1
Materials and Methods
Figs. S1 to S3
Tables S1 and S2
References

25 April 2006; accepted 21 July 2006
10.1126/science.1129161

Plant Genotypic Diversity Predicts Community Structure and Governs an Ecosystem Process

Gregory M. Crutsinger,^{1*} Michael D. Collins,¹ James A. Fordyce,¹ Zachariah Gompert,² Chris C. Nice,² Nathan J. Sanders¹

Theory predicts, and recent empirical studies have shown, that the diversity of plant species determines the diversity of associated herbivores and mediates ecosystem processes, such as aboveground net primary productivity (ANPP). However, an often-overlooked component of plant diversity, namely population genotypic diversity, may also have wide-ranging effects on community structure and ecosystem processes. We showed experimentally that increasing population genotypic diversity in a dominant old-field plant species, *Solidago altissima*, determined arthropod diversity and community structure and increased ANPP. The effects of genotypic diversity on arthropod diversity and ANPP were comparable to the effects of plant species diversity measured in other studies.

Ecological theory (1, 2) and field experiments (3, 4) have revealed a positive relationship between the diversity of plant species and the diversity of associated consumers. At least two mechanisms might explain this pattern. First, because approximately 90% of herbivorous insects exhibit some degree of host specialization (5), as plant species richness increases, so should the number of associated herbivore species. This resource specialization hypothesis has some theoretical support (1, 2, 6). Second, if aboveground net primary productivity (ANPP) increases as plant species richness increases (7), then more herbivore individuals, and therefore more species, will be supported by increases in available energy (this has been called the more individuals hypothesis) (8). An increase in the number of herbivore species by either of these mechanisms should support more predator species (9). Recent studies have

shown that population genotypic diversity, like plant species diversity, can have extended consequences for communities and ecosystems (10–14). However, no studies to date have explicitly linked intraspecific genotypic diversity, the structure of associated communities, and the potential mechanisms driving these patterns, such as energy availability. This paucity of studies exists despite numerous calls for such research within the literature regarding biodiversity-ecosystem function (7, 15). We tested whether host-plant genotypic diversity determines the structure of associated arthropod communities and governs an ecosystem process, ANPP, that influences arthropod species richness.

We manipulated the plot-level genotypic diversity (the number of genotypes per plot) of *Solidago altissima*, tall goldenrod, a common perennial plant throughout eastern North America. Twenty-one *S. altissima* ramets were collected from local *S. altissima* patches growing in fields near the study site, and each ramet was identified as a unique genotype by means of amplified fragment length polymorphism. From these 21 genotypes, we established 63 1-m² experimental plots, each containing 12 individ-

uals and 1, 3, 6, or 12 randomly selected genotypes, mimicking the densities and levels of genotypic diversity found in natural patches of similar size. We censused arthropods on every ramet in each plot five times over the course of the growing season. In total, we counted 36,997 individuals of ~136 species. We estimated ANPP at the peak of the growing season using nondestructive allometric techniques (16).

Total cumulative arthropod species richness increased with plant genotypic diversity. The number of arthropod species was, on average, 27% greater in 12-genotype plots than in single-genotype plots (Fig. 1), indicating that plant genotypic diversity was an important determinant of arthropod diversity. When we examined the effects of genotypic diversity on community structure, we found that herbivore species richness (Fig. 2B) and predator richness (Fig. 2A) also increased with increasing genotypic diversity. The effects of genotypic diversity on arthropod communities were nonadditive (Fig. 1). That is, total arthropod richness and herbivore and predator richness were all greater in the 6- and 12-genotype plots than would be predicted by summing the number of arthropod species associated with the corresponding genotypes grown in monoculture ($P < 0.01$).

ANPP also increased with plant genotypic diversity and was 36% greater in 12-genotype plots than in single-genotype plots (Fig. 2C). The effect of genotypic diversity on ANPP could be due to increased niche complementarity (mixed genotypes used available resources more completely or mixed genotypes facilitated one another, thereby increasing ANPP in mixtures) (7, 15) or to sampling or selection effects (increased ANPP caused by randomly assembled mixtures having a higher probability of containing highly productive genotypes) (17). Using standard techniques (18) we found that selection effects were highly variable and were not significantly different from zero ($P > 0.60$ for all treatments), indicating that highly productive genotypes do not dominate in mixtures and drive observed increases in ANPP. Selection

¹Department of Ecology and Evolutionary Biology, University of Tennessee, Knoxville, TN 37996, USA. ²Department of Biology, Texas State University, San Marcos, TX 78666, USA.

*To whom correspondence should be addressed. E-mail: gcrutsin@utk.edu